

## Vasorelaxant effect of a phenylethylamine analogue based on schwarzinicine A an alkaloid isolated from the leaves of *Ficus schwarzii*

Kayatri Govindaraju<sup>a</sup>, Yin Ying Mak<sup>b</sup>, Fong Kai Lee<sup>c</sup>, Claudia C. Bauer<sup>d</sup>, Kuan Hon Lim<sup>b</sup>, Robin S. Bon<sup>d</sup>, Cin Kong<sup>b</sup>, Sue Mian Then<sup>b</sup>, Kang Nee Ting<sup>b,\*</sup>,<sup>1</sup>

<sup>a</sup> Faculty of Pharmacy, Universiti Malaya, Jln Profesor Diraja Ungku Aziz, 50603, Kuala Lumpur, Malaysia

<sup>b</sup> School of Pharmacy, University of Nottingham Malaysia, Jln Broga, 43500 Semenyih, Selangor, Malaysia

<sup>c</sup> Faculty of Pharmacy and Biomedical Sciences, MAHSA University, Jln SP 2, Bandar Saujana Putra, 42610 Jenjarom, Selangor, Malaysia

<sup>d</sup> Department of Discovery and Translational Science Department, Leeds Institute of Cardiovascular and Metabolic Medicine, University of Leeds, UK

### ARTICLE INFO

#### Keywords:

Schwarzinicine A  
Phenylethylamine  
Vascular smooth muscle  
Vasodilator  
TRPC cation channels

### ABSTRACT

**N**-Phenethyl-1-phenyl-pentan-3-amine (**1**) is a new compound synthesised as a simplified analogue of schwarzinicine A (**2**), a natural compound extracted from *Ficus schwarzii*. Compound **1** differs from compound **2** due to its structural simplification, featuring two phenyl rings without methoxy substitution, as opposed to compound **2**, which possesses three 3,4-dimethoxy aromatic rings. Our previous research findings highlighted the calcium-inhibitory effects of compound **2**, but the mechanism of action for compound **1** remains unexplored, serving as the primary focus of this study. Building upon our earlier research, this study aimed to elucidate compound **1**'s calcium-modulating potential by using rat-isolated aortae in an organ bath set-up and HEK cells expressing hTRPC channels with the fluorometric assay to measure calcium influx. Compound **1** elicited a vasorelaxation response ( $E_{\max}$  111.4%) similar to its parent compound **2** ( $E_{\max}$  123.1%), and inhibited hTRPC3-, hTRPC4-, hTRPC5-, and hTRPC6-mediated calcium influx into HEK cells with  $IC_{50}$  values of 6, 2, 2, 5  $\mu$ M, respectively. Compound **1** has a similar pharmacological profile as its parent compound **2**, whereby it exerts a vasorelaxant effect by attenuating calcium influx and inhibits multiple TRPC channels.

### 1. Introduction

*Ficus schwarzii* latex has been used traditionally for the treatment of ringworm infections (Asian Tropical Plant, 2014). From our earlier work, we have identified a series of 1,4-diarylbutanoid-phenethylamine conjugates (schwarzinicines A-G) from the leaves of *Ficus schwarzii*. In particular, schwarzinicine A (**2**) displayed significant vasorelaxation effects in the rat-isolated aorta (Krishnan et al., 2020; Mak et al., 2022). However, the low isolation yields of these alkaloids (0.00002–0.00180%, based on dry weight) precluded further pharmacological investigations. In an attempt to explore synthetically accessible analogues, we synthesised **N**-phenethyl-1-phenyl-pentan-3-amine (**1**) as a new simplified analogue. Both compounds **1** and **2** exhibit similar structural features, including an arylethyl fragment connecting to an arylpropyl fragment through a secondary amine N, as well as a chiral centre at the same position (Fig. 1). However, there are notable differences between the two compounds. Compound **2** is characterised

by three 3,4-dimethoxy-substituted aromatic rings, while compound **1** comprises two phenyl rings without methoxy substitution. Their molecular weight is 509.63 and 267.41, respectively.

The transient receptor potential (TRP) family is the latest cation channel widely discussed, and they are found expressed in several vascular beds. The intricate interplay between  $Ca^{2+}$  signalling and TRP channels emerges as a pivotal regulator of the transition from a healthy physiological phenotype to a pathological state in vascular smooth muscle cells (VSMCs) (Earley and Brayden, 2015). Among the TRP channels, TRPC (canonical) and TRPV (vanilloid) isoforms have emerged as key regulators of vascular dynamics (Martín-Bórnez et al., 2020). The TRPC family comprises 7 members and is divided into three clusters (TRPC1/4/5, TRPC2, and TRPC3/6/7) (Wang et al., 2020), all of which are expressed in humans except for TRPC2 (Minard et al., 2019; Vannier et al., 1999; Wes et al., 1995). TRPC channels play a vital role in  $Ca^{2+}$  influx in vascular cells and are implicated in various physiological and pathological processes (Abramowitz and Birnbaumer, 2009; Bon

\* Correspondence to: School of Pharmacy, University of Nottingham, Malaysia Campus, Jln Broga, 43500 Semenyih, Selangor, Malaysia.

E-mail address: [Kang-Nee.Ting@nottingham.edu.my](mailto:Kang-Nee.Ting@nottingham.edu.my) (K.N. Ting).

<sup>1</sup> ORCID: <https://orcid.org/0000-0002-7818-3922>

<https://doi.org/10.1016/j.phytol.2023.11.007>

Received 9 September 2023; Received in revised form 23 November 2023; Accepted 26 November 2023

Available online 9 December 2023

1874-3900/© 2023 The Author(s). Published by Elsevier Ltd on behalf of Phytochemical Society of Europe. This is an open access article under the CC BY license (<http://creativecommons.org/licenses/by/4.0/>).

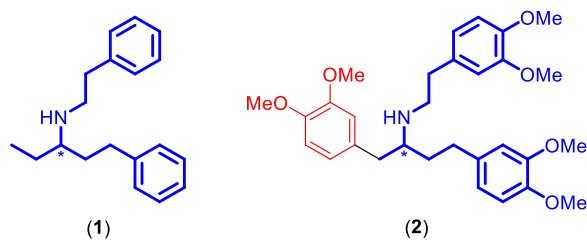


**Fig. 1.** Chemical structures of *N*-phenethyl-1-phenyl-pentan-3-amine (1) and schwarzinicine A (2). The common structural elements are highlighted in bold. 1 was synthesised as a racemic mixture, while 2 was obtained naturally as a salemic mixture (4:1 ratio of (+)/(-)).

et al., 2022; Martín-Bórnez et al., 2020). Meanwhile, only a few reports have studied the role of TRPV in vascular tone regulation, and most of them have demonstrated their relevance in relation to endothelium function.

Although the physiological contributions of TRPC channels to cardiovascular cellular function are still being discovered, unequivocal evidence exists for their involvement in models of cardiovascular disease, prompting the pursuit of TRPC channel modulators as potential therapeutics. TRPC channel isoforms have been implicated in hypertension-related vascular remodelling and heightened vasoconstriction (Earley and Brayden, 2015; Grayson et al., 2017). These responses are mainly attributable to the alteration of  $\text{Ca}^{2+}$  and VSMC proliferation (Liu et al., 2014). Studies involving mouse models of essential hypertension or spontaneously hypertensive rats have consistently reported significant upregulation of TRPC isoforms in key arteries (Álvarez-Miguel et al., 2017; Earley and Brayden, 2015; Lin et al., 2015). Among these, TRPC3/6 channels have been extensively studied and are associated with regulating blood pressure and hypertension development in both animals and humans (Chen et al., 2010; Dietrich et al., 2005; Earley and Brayden, 2015; Liu et al., 2005; Thilo et al., 2009). TRPC4 and TRPC5 channels, expressed in various smooth muscle cell types, function as store-operated channels with moderate to high calcium permeabilities, contributing significantly to blood vessel tone regulation. However, their exact role in the store-operated calcium entry (SOCE) pathway remains to be fully elucidated.

Our structure-activity relationship study based on the structure of compound 2 revealed that the methoxy groups have negligible impact on its activity (Lee et al., 2022). Moreover, we determined that only two out of the three aromatic rings in 1 are sufficient for its activity. Notably, our previously published data emphasise the inhibitory effects of 2 on TRPC channels (Mak et al., 2022). This study aimed to investigate the role of compound 1 in modulating calcium using rat-isolated aortae and HEK cells expressing hTRPC channels.

## 2. Material and methods

### 2.1. Tissue preparation

Male Sprague Dawley rats (235–440 g; 6–8 weeks old) were purchased from the University Putra Malaysia (UPM) and Universiti Kebangsaan Malaysia (UKM). Sprague Dawley rats are known to express TRPC 3, 4, 5 and 6 in their aorta (Facemire et al., 2004). All animals were randomly divided for each protocol ( $\geq 4$  rats/ protocol). The isolation of rat aortae was adapted from previously described methods (Loong et al., 2015). All tissues were then stimulated twice with 60 mM potassium chloride (KCl) to check their reactivity and viability.

### 2.2. Drugs, chemicals, and media

(R)-(-)-Phenylephrine hydrochloride (Sigma Aldrich, UK), potassium chloride (KCl), nifedipine (Nacalei Tesque, Japan), 1-[2-(4-methoxyphenyl)-2-[3-(4-methoxyphenyl)propoxy]ethyl]imidazole

(SKF96365; Sigma, UK), *L*- $N^G$ -nitroarginine methyl ester (*L*-NAME; Tocris Bioscience, UK), ethyl-1-(4-(2,3,3-trichloroacrylamide)phenyl)-5-(trifluoromethyl)-1*H*-pyrazole-4-carboxylate (Pyr3; Sigma, USA), HC-070 (Just et al., 2018), sodium nitroprusside (SNP; Sigma, USA), tetraethylammonium chloride (TEA; Sigma, USA), 4-aminopyridine (4-AP; Tocris Bioscience, UK), isobutylmethylxanthine (IBMX; Tocris Bioscience, UK), ethylenebis(oxyethylenenitrilo)]tetraacetic acid (EGTA; Sigma, USA). All compounds tested in assays were dissolved in dimethyl sulfoxide (DMSO) except phenylephrine, *L*-NAME, and SNP, which were dissolved in water. Lower concentrations of 1 (0.1–30 mM; MW: 267.41 g/mol) were diluted accordingly from 100 mM stock solutions using 100% DMSO.

To make standard buffer solution (SBS), sodium chloride (NaCl; Fisher Scientific, Belgium), potassium chloride (KCl; Honeywell, Germany), calcium chloride ( $\text{CaCl}_2$ ; Sigma-Aldrich, Japan), magnesium chloride ( $\text{MgCl}_2$ ; Sigma-Aldrich, Japan), *D*-(+)-glucose (Sigma-Aldrich, USA), HEPES (Fisher Scientific, Taiwan) were used. Fura-2 acetoxymethyl ester (fura-2 AM; Invitrogen, UK) and 1-oleoyl-2-acetyl-*sn*-glycerol (OAG; Sigma) were dissolved in DMSO (Honeywell, Germany) to make a stock solution of 1 mM and 100 mM, respectively. 10% pluronic acid (Sigma, USA) dissolved in DMSO was diluted 1:1000 to fura-2 AM containing SBS to facilitate the loading of fura-2 AM into the cells. Sphingosine-1-phosphate (S1P; Merck, UK) was dissolved in methanol to 5 mM and stored at  $-80^\circ\text{C}$ .

### 2.3. Synthesis of *N*-Phenethyl-1-phenyl-pentan-3-amine

#### 2.3.1. *N*-Methoxy-*N*-methylpropionamide (4)

Propionyl chloride (3) (2.01 g, 21.7 mmol, 1 equiv.) was added dropwise into a mixture of *N*,*O*-dimethylhydroxylamine hydrochloride (2.32 g, 23.8 mmol, 1.1 equiv) and pyridine (4.4 mL, 54.4 mmol, 2.5 equiv) in  $\text{CH}_2\text{Cl}_2$  (20 mL) in an ice bath. The reaction mixture was allowed to warm to room temperature and stir at this temperature for 2.5 h. It was then diluted with EtOAc (40 mL), washed with 1 M HCl solution ( $2 \times 40$  mL), followed by saturated aq.  $\text{KHCO}_3$  solution ( $2 \times 40$  mL) and finally brine (40 mL). The organic layer was dried over  $\text{MgSO}_4$  and concentrated in vacuo to yield *N*-methoxy-*N*-methylpropionamide (4) as a colourless oil (912.6 mg, 7.79 mmol, 36%). The product was used in the next reaction without further purification. IR (neat):  $\nu_{\text{max}}$  2979, 2942, 1664, 1380, 1180, 1010  $\text{cm}^{-1}$ ;  $^1\text{H}$  NMR ( $\text{CDCl}_3$ , 700 MHz):  $\delta$  3.69 (s, 3 H), 3.19 (s, 3 H), 2.46 (q,  $J = 7.6$  Hz, 2 H), 1.14 (t,  $J = 7.5$  Hz, 3 H);  $^{13}\text{C}$  NMR ( $\text{CDCl}_3$ , 175 MHz):  $\delta$  175.6, 61.2, 32.3, 25.2, 8.8; HRESIMS  $m/z$  118.0870 [ $\text{M} + \text{H}$ ] $^+$  (calcd for  $\text{C}_5\text{H}_{12}\text{NO}_2$ , 118.0868). The spectroscopic data are in good agreement with those reported in the literature (Kerr et al., 2012).

#### 2.3.2. 1-Phenylpentan-3-one (5)

To an ice-cold solution of *N*-methoxy-*N*-methylpropionamide (4) (402.8 mg, 3.44 mmol, 1 equiv.) in THF (12 mL) was added dropwise a solution of phenethylmagnesium chloride (1.0 M in THF) (15 mL, 15.0 mmol, 4.4 equiv). The reaction mixture was stirred in an ice bath for 2.5 h prior to addition of cold 10% HCl solution (20 mL). After stirring for 5 min, the mixture was extracted with EtOAc ( $3 \times 30$  mL). The combined organic layers were washed with water (20 mL) and brine (20 mL) before drying with  $\text{MgSO}_4$  and concentrated in vacuo. The crude product was purified by centrifugal radial TLC using an eluent system of  $\text{Et}_2\text{O}$ -hexane (1:5) to yield 1-phenylpentan-3-one (5) as a colourless oil (420.6 mg, 2.59 mmol, 75%). IR (neat):  $\nu_{\text{max}}$  3063, 3028, 2977, 2938, 1717, 1497, 1454, 1113  $\text{cm}^{-1}$ ;  $^1\text{H}$  NMR ( $\text{CDCl}_3$ , 700 MHz):  $\delta$  7.14–7.32 (m, 5 H), 2.90 (t,  $J = 7.7$  Hz, 2 H), 2.73 (t,  $J = 7.8$  Hz, 2 H), 2.40 (q,  $J = 7.3$  Hz, 2 H), 1.04 (t,  $J = 7.4$  Hz, 3 H);  $^{13}\text{C}$  NMR ( $\text{CDCl}_3$ , 175 MHz):  $\delta$  210.7, 141.2, 128.5, 128.3, 126.1, 43.9, 36.1, 29.9, 7.8; HRESIMS  $m/z$  163.1130 [ $\text{M} + \text{H}$ ] $^+$  (calcd for  $\text{C}_{11}\text{H}_{15}\text{O}$ , 163.1123). The spectroscopic data are in good agreement with those reported in the literature (Huang et al., 2015).

### 2.3.3. *N*-Phenethyl-1-phenylpentan-3-amine (1)

To a stirring solution of 1-phenylpentan-3-one (**5**) (206.3 mg, 1.27 mmol, 1 equiv) in  $\text{ClCH}_2\text{CH}_2\text{Cl}$  (5 mL) was added phenethylamine (0.17 mL, 1.38 mmol, 1.1 equiv),  $\text{NaBH}(\text{OAc})_3$  (431.8 mg, 2.04 mmol, 1.6 equiv) and  $\text{AcOH}$  (0.075 mL, 1.31 mmol, 1 equiv). The solution was stirred at room temperature for 22 h before the addition of 1 M  $\text{NaOH}$  solution (9 mL). The mixture was then extracted with  $\text{EtOAc}$  ( $3 \times 10$  mL). The combined organic layers were washed with brine (10 mL) and subsequently dried with  $\text{Na}_2\text{SO}_4$  before being concentrated in vacuo. The crude product was purified by centrifugal radial TLC using an eluent system of  $\text{Et}_2\text{O}$ –hexane (1:5) to yield *N*-phenethyl-1-phenylpentan-3-amine (**1**) as a yellow oil (245.6 mg, 0.92 mmol, 72%). The purity of *N*-phenethyl-1-phenylpentan-3-amine was at least 99% by NMR. IR (neat):  $\nu_{\text{max}}$  3326, 3026, 2930, 1603, 1495, 1454, 1139, 1030  $\text{cm}^{-1}$ ;  $^1\text{H}$  NMR ( $\text{CDCl}_3$ , 600 MHz):  $\delta$  7.33 – 7.09 (m, 10 H), 2.90 – 2.79 (m, 2 H), 2.79 – 2.72 (m, 2 H), 2.60 – 2.50 (m, 2 H), 2.50 – 2.42 (m, 1 H), 1.72 – 1.63 (m, 2 H), 1.49 – 1.41 (m, 2 H), 0.86 – 0.81 (m, 3 H) (Supplementary data, Fig. S1);  $^{13}\text{C}$  NMR ( $\text{CDCl}_3$ , 150 MHz):  $\delta$  142.6, 140.3, 128.7, 128.5, 128.4, 126.2, 125.7, 58.2, 48.2, 36.7, 35.3, 32.1, 26.3, 9.8 (Supplementary data, Fig. S2); HRESIMS  $m/z$  268.2057 [ $\text{M} + \text{H}$ ]<sup>+</sup> (calcd for  $\text{C}_{19}\text{H}_{26}\text{N}$ , 268.2065).

## 2.4. Functional characterisation of compound 1 using rat-isolated aortic rings

### 2.4.1. Vasorelaxant effect of compound 1

To investigate the vasorelaxant activity of **1**, **2** and other known drugs, nifedipine, SKF96365, Pyr3 and HC-070 on rat aortae, the aortic rings were pre-constricted with phenylephrine (0.1  $\mu\text{M}$ ). Once a stable tone was established, concentration-response curves were constructed for each compound. The concentration range used was between 1 nM and 100  $\mu\text{M}$  for all the drugs except HC-070 (1 nM to 30  $\mu\text{M}$ ). One concentration-response curve was performed per tissue.

### 2.4.2. Effects of endothelium and nitric oxide (NO) on compound 1-induced relaxation

To investigate the involvement of endothelium, **1** was applied cumulatively on endothelium-denuded aortic tissues that were pre-constricted with phenylephrine. The denudation of aortic rings was achieved by a surface abrasion method, whereby the endothelium is removed mechanically by gently rolling the lumen of the aortic rings using the blunt tip of stainless-steel forceps (Gokce and Arun, 2014; Idris et al., 2015). The endothelial integrity and functional removal were verified by the presence or absence of the relaxant response to carbachol (1  $\mu\text{M}$ ) on the phenylephrine (0.1  $\mu\text{M}$ ) contracted aortic rings. The concentrations of carbachol and phenylephrine were chosen on the basis of their ability to cause at least 70% relaxation (carbachol) and contraction (phenylephrine), which were determined from their respective concentration-response curves. The aortic rings were considered intact if the relaxation induced by carbachol was greater than 80%, and the aortic rings were assumed to be denuded if the relaxation was less than 10% (Arsyad and Dobson, 2016).

In a separate experiment, in order to further confirm the involvement of endothelium-derived factors on **1**-induced relaxation, L-NAME (a nitric oxide synthase inhibitor) and SNP (a nitric oxide donor) were used. The endothelium-denuded rings were incubated with L-NAME (100  $\mu\text{M}$ ), prior to performing **1** concentration-response measurement in aortic rings pre-constricted with phenylephrine (0.1  $\mu\text{M}$ ). The concentration range of **1** used was between 1 nM and 100  $\mu\text{M}$ .

For SNP, the endothelium intact aortic rings were incubated with **1** (30  $\mu\text{M}$ ) followed by cumulative addition of SNP in aortic rings pre-constricted with phenylephrine (0.1  $\mu\text{M}$ ). The concentration range of SNP used was between 0.01 nM and 1  $\mu\text{M}$ .

### 2.4.3. Effects of adrenergic receptor antagonists, phosphodiesterase inhibitor and potassium channel blockers on compound 1-induced relaxation

To investigate whether **1** was blocking  $\alpha$ -adrenergic receptors, prazosin ( $\alpha_1$ -adrenergic receptor antagonist, 10  $\mu\text{M}$ ), or rauwolscine ( $\alpha_2$ -adrenergic receptor antagonist, 10  $\mu\text{M}$ ), was added to the bath for 30 min prior to the construction of the concentration-response curve of **1**. For this set of protocols, the aortic rings were pre-constricted with 60 mM KCl. To determine the role of  $\beta$ -adrenergic receptors, propranolol and timolol (non-selective  $\beta$ -adrenergic receptor antagonist, 3  $\mu\text{M}$ ), were applied prior to performing the **1** concentration-response curve (1 nM and 300  $\mu\text{M}$ ).

The involvement of cGMP / cAMP in the relaxation by **1** was examined using a non-selective phosphodiesterase (PDE) inhibitor, isobutylmethylxanthine (IBMX). The aortic rings were incubated with IBMX (10  $\mu\text{M}$ ) for 40 min, followed by cumulative addition of **1** in aortic rings pre-constricted with phenylephrine (0.1  $\mu\text{M}$ ). The concentration range of **1** used was between 1 nM and 300  $\mu\text{M}$ . To investigate the involvement of potassium channels in the relaxation of **1**, potassium channel inhibitors, TEA (calcium-activated potassium channel,  $\text{K}_{\text{Ca}}$  inhibitor) and 4-AP (voltage-gated potassium channel,  $\text{K}_v$  inhibitor) were used (Panthiya et al., 2019; Tammaro et al., 2004). The aortic rings were incubated with TEA (3 mM) and 4-AP (1 mM) for 40 min, followed by cumulative addition of **1** in aortic rings pre-constricted with phenylephrine (0.1  $\mu\text{M}$ ).

### 2.4.4. Effect of compound 1 on L-type and T-type $\text{Ca}^{2+}$ channels

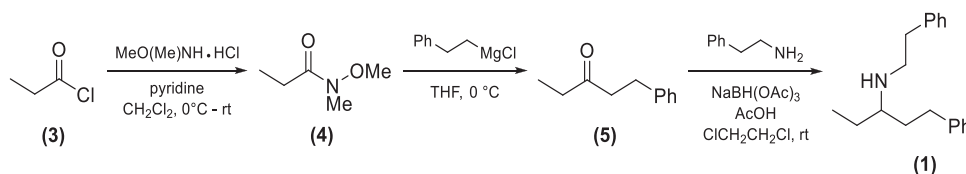
The involvement of L-type  $\text{Ca}^{2+}$  channels in compound **1**-induced relaxation was tested by pre-incubating the aortic rings with nifedipine (30  $\mu\text{M}$ ) for 40 min. Then, the rings were pre-constricted with PE (0.1  $\mu\text{M}$ ) prior to performing the **1** concentration-response curve.

To further investigate the involvement of L-type  $\text{Ca}^{2+}$  channels, following the second KCl stimulation, tissues were washed with a normal Krebs-Ringer solution. Then, they were treated with a single concentration of PE (10  $\mu\text{M}$ ). Once the response had stabilised, the tissues were washed for 15 mins. The tissues were then incubated with nifedipine (30  $\mu\text{M}$ ) for 40 min, followed by the addition of a single concentration of PE (10  $\mu\text{M}$ ). After that, a single concentration of **1** (30  $\mu\text{M}$ ) was added to the bath and left for 1 h. The concentration of nifedipine and **1** used in this experiment were chosen based on their ( $\text{IC}_{50}$ ) ability to cause 90%–100% relaxation in rat aorta.

The involvement of T-type  $\text{Ca}^{2+}$  channels in **1**-induced relaxation was tested using verapamil (Bergson et al., 2011). Firstly, the aortic rings were pre-incubated with verapamil (30  $\mu\text{M}$ ) for 40 min. Then, the rings were pre-constricted with PE (0.1  $\mu\text{M}$ ) prior to performing **1** CRC. To further investigate the involvement of T-type  $\text{Ca}^{2+}$  channels, following the second KCl stimulation, tissues were washed with a normal Krebs-Ringer solution. Then, they were treated with a single concentration of PE (10  $\mu\text{M}$ ). Once the response had stabilised, the tissues were washed for 15 mins. The tissues were then incubated with verapamil (30  $\mu\text{M}$ ) for 40 min, followed by the addition of a single concentration of PE (10  $\mu\text{M}$ ). Thereafter, a single concentration of **1** (30  $\mu\text{M}$ ) was added to the bath and left for 1 h. The concentrations of verapamil and **1** used in this experiment were chosen based on their ability to cause 100% relaxation in the rat aorta.

### 2.4.5. Effect of compound 1 on $\text{CaCl}_2$ -induced contraction in $\text{Ca}^{2+}$ -free Krebs solution

To investigate the concentration-dependent effect of **1** on  $\text{CaCl}_2$ -induced contraction, the tissues were equilibrated for 30 min in a calcium-free Krebs solution. Then, the tissues were pre-incubated with **1** (10  $\mu\text{M}$  or 30  $\mu\text{M}$ ) for 40 min. This was then followed by adding 60 mM KCl to confirm the viability of tissues in  $\text{Ca}^{2+}$ -free Krebs solution. Once the KCl-induced contractile response plateaued, a concentration-response curve to  $\text{CaCl}_2$  was constructed. The concentration range of  $\text{CaCl}_2$  used was between 0.1  $\mu\text{M}$  and 3 mM.



**Scheme 1.** Synthesis of *N*-phenethyl-1-phenylpentan-3-amine (**1**).

#### 2.4.6. Effect of compound **1** on stored $Ca^{2+}$

To investigate the effect of **1** on stored calcium, the tissues were washed with a  $Ca^{2+}$ -free Krebs-Ringer solution. Then, they were incubated with **1** (30  $\mu$ M) for 40 min, followed by the addition of EGTA (10  $\mu$ M) into the bath for 10 min before stimulating the tissues with a single concentration of phenylephrine (10  $\mu$ M) and left for 1 h (Guan et al., 1988; Low et al., 1992).

#### 2.5. Intracellular $Ca^{2+}$ measurements

##### 2.5.1. Cell culture

To study the inhibitory role of **1** against TRPC channels, HEK 293 cells overexpressing human TRPC channels (TRPC3, TRPC4, TRPC5 or TRPC6) were used. Wild-type (WT) HEK 293 cells, and (Tet+) HEK T-REx™ cells expressing either human TRPC3, TRPC4 or TRPC5 were cultured in 75 cm<sup>2</sup> flasks in DMEM GlutaMAX™ (Invitrogen, Paisley, UK), supplemented with 10% FBS (Sigma-Aldrich) and 100 units/mL, 100  $\mu$ g/mL penicillin-streptomycin (ThermoFisher Scientific, UK). HEK T-REx™ cells expressing TRPC channels were supplemented with the addition of blasticidin (10  $\mu$ g/mL) and zeocin (400  $\mu$ g/mL; Invivogen, San Diego, California, USA) to maintain stable expression of the tetracycline repressor protein and relevant TRPC channel (Akbulut et al., 2015; Ludlow et al., 2017; Minard et al., 2019; Rubaiy et al., 2017). TRPC protein expression was induced with 1  $\mu$ g/mL tetracycline 24 h before recording. Cells were passaged 1:10 every 3–4 days by washing with 10 mL PBS (Sigma, USA) followed by 2 mL pre-warmed trypsin (0.25%, ThermoFisher Scientific). Cells were maintained in a humidified incubator with 5% CO<sub>2</sub> at 37 °C. For experiments using hTRPC6, wild-type (WT) HEK 293 cells were transfected with hTRPC6 (cloned into pcDNA3) using jetPRIME® transfection reagent (VWR, Lutterworth, UK) (Mak et al., 2022; Minard et al., 2019). Transfected cells were plated 24 h after transfection. Assays were then carried out 24 h after plating.

##### 2.5.2. Fluorometric $[Ca^{2+}]_i$ recordings

$[Ca^{2+}]_i$  recordings were carried out on FlexStation 3 Multimode Microplate Reader (Molecular Devices, San Jose, CA). Cells were incubated with 2  $\mu$ M Fura-2 AM in SBS containing 0.01% pluronic acid for 60 min at 37 °C. After washing twice with SBS, cells were incubated with recording buffer (SBS containing **1** or DMSO 0.1%) for 30 min at room temperature before commencing recordings. Dual excitation wavelengths (340 and 380 nm) and an emission wavelength of 510 nm were used in the experiment. Measurements were taken every 5 s for 5 min at room temperature. Baseline recordings were measured at the beginning from 0 to 55 s. At 60 s, 80  $\mu$ L of compound buffer containing 200  $\mu$ M OAG (TRPC3/6 channel activator) or 10  $\mu$ M S1P (TRPC4/5 activator) was automatically pipetted from the compound plate to the cell plate. Compound **1** or DMSO 0.1% were previously added to the compound buffer preparation to maintain concentration on cells after compound addition. For TRPC3 and TRPC6 experiments, 0.01% pluronic acid was added to the recording and compound buffers. Each fluorometric  $[Ca^{2+}]_i$  experiment consisted of six technical replicates (six wells on each row of a 96-well plate), represented by N = 6. The methods used in cell culture, transfection and fluorometric  $[Ca^{2+}]_i$  recordings were adopted from Minard et al. (Minard et al., 2019).

#### 2.6. Statistical analysis

All data were expressed as mean  $\pm$  SEM of *n* number of animals in the isometric tension recording experiment. The relaxation responses were expressed as percentage inhibition of the respective contractile agonist-induced contraction. Maximum response ( $E_{max}$ ) and  $EC_{50}$  were obtained from the non-linear regression fit curve.  $pEC_{50}$  (negative logarithm of  $EC_{50}$ ) values were also determined. In experiments where  $E_{max}$  was not achieved, the maximum response was calculated as the percentage of relaxation at the highest concentration tested. For fluorometric  $[Ca^{2+}]_i$  recordings, *n* is the number of independent experiments performed on cultured cells. The amplitude of intracellular  $Ca^{2+}$  recordings was measured from 90 to 140 s (TRPC3 and TRPC6), 110–130 s (TRPC4), or 150–180 s (TRPC5), respectively. Data were normalised to the response in the activator control to remove unwanted variation. Concentration-response curves were fitted with a 3-parameter non-linear regression fit with the maximum activity defined as 100%.  $IC_{50}$  values for TRPC3/4/5/6 channels were obtained from the curve fit.

Unpaired Student's *t*-test was used to compare the vehicle control and treatment group. In the multi-group analysis, one-way ANOVA followed by Dunnett's multiple comparisons test was used when F in ANOVA was significant ( $p < 0.05$ ), and there was no variance inhomogeneity. Data were analysed using GraphPad Prism Version 8.2.1 (La Jolla, California, USA). A probability of less than 0.05 ( $p < 0.05$ ) was considered statistically significant, indicated by asterisks: \*  $p < 0.05$ ; \*\*  $p < 0.01$ ; \*\*\*  $p < 0.001$ , \*\*\*\*  $p < 0.0001$ .

### 3. Results

#### 3.1. Synthesis of compound **1**

*N*-phenethyl-1-phenylpentan-3-amine (**1**) was synthesised as a simplified analogue of schwarzinicine A (**2**). As illustrated in Scheme 1, the synthesis of **1** commenced with the conversion of the commercially available propionyl chloride (**3**) to its corresponding Weinreb amide (**4**), which was subsequently allowed to react with phenethylmagnesium chloride to yield ketone (**5**) in 75% yield. Finally, reductive amination of ketone (**5**) with  $NaBH(OAc)_3$  in the presence of phenethylamine furnished **1** in 72% yield. All synthesised compounds were characterised by <sup>1</sup>H NMR, <sup>13</sup>C NMR, IR and HRESIMS and the data are reported in the Materials and Methods section. The final compound (a racemic mixture) was analytically pure according to <sup>1</sup>H NMR and <sup>13</sup>C NMR analysis (Supplementary data, Fig. S1 and S2).

#### 3.2. Compound **1** shows relaxation responses similar to the non-selective TRPC channel inhibitor SKF96365

The relaxation effect of **1** in rat aorta was compared with **2**, SKF96365, nifedipine, Pyr3 (a selective TRPC3 channel inhibitor) and HC-070 (a selective, nanomolar TRPC4/5 channel inhibitor with micromolar activity against TRPC3). Compound **1** at higher concentrations, is capable of inducing complete relaxation at the highest concentration, similar to its parent compound **2** and SKF96365 with similar potency (Fig. 2, Table 1), with significantly better efficacy than Pyr3 but not HC-070. Interestingly, although nifedipine shows a slightly better potency, it has marginally lower efficacy than **1**, **2** and SKF96365.

N/A non-applicable.

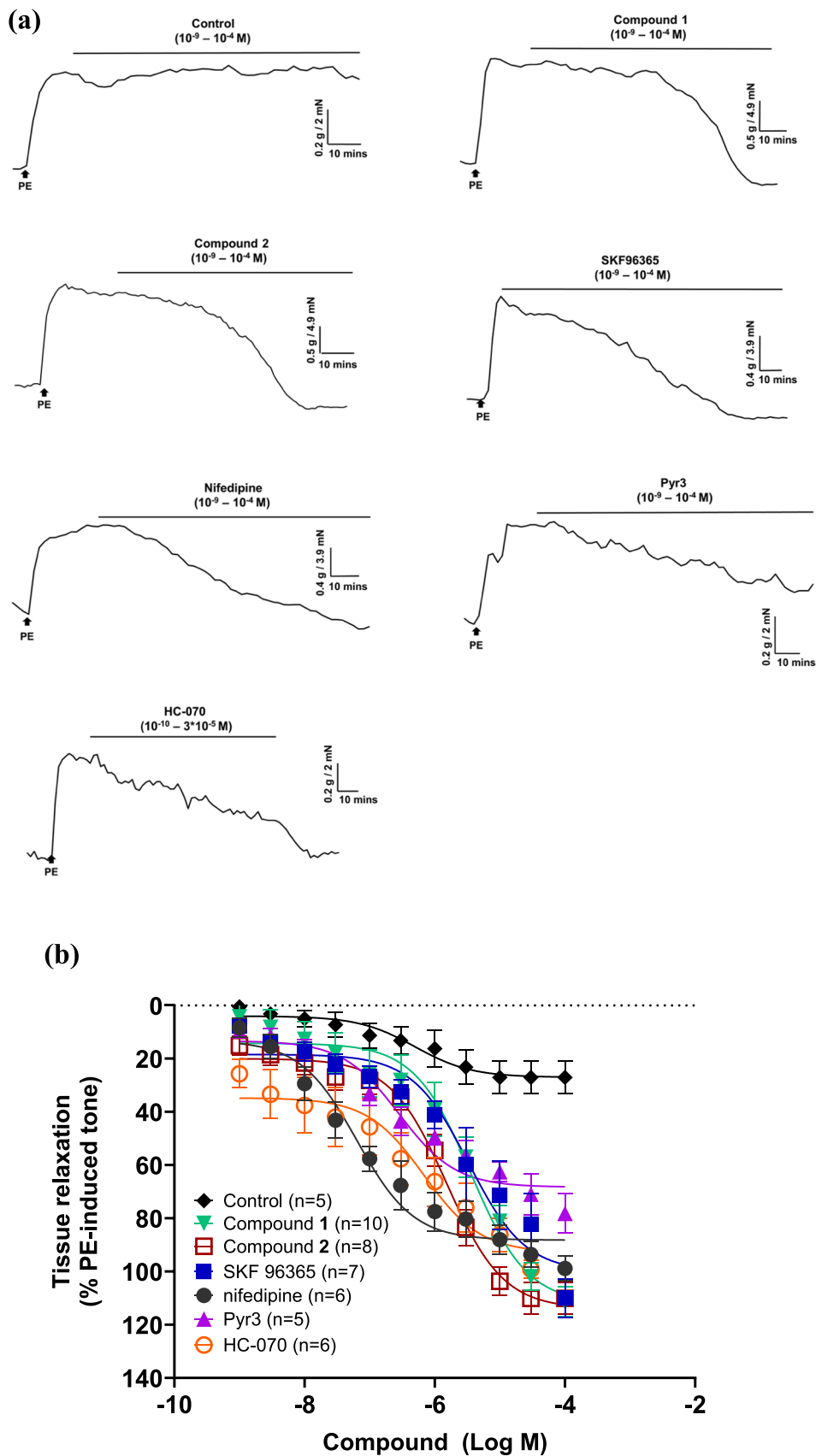


**Fig. 2.** (a) Representative trace recording of the effects of DMSO (vehicle control), Compound 1, Compound 2, SKF96365, nifedipine, Pyr3 and HC-070 against rat-isolated aortic rings pre-contracted with phenylephrine. The concentration-response curves of all the compounds studied are shown in (b). Tissue relaxations were expressed as the percentage of phenylephrine-induced contraction. Data are presented as mean values  $\pm$  SEM of n number of animals. PE, phenylephrine.

**Table 1**

Vasorelaxation effects of compound 1, compound 2 and other calcium channel inhibitors. The values are the mean  $\pm$  SEM of  $n$  number of animals.

	$E_{\max}$ (%)	$p$ -value	Relative ( $E_{\max}$ ) <sup>b</sup>	$pEC_{50}$	$p$ -value
Control	27.1 $\pm$ 6.0**** <sup>a</sup>	<0.0001	0.2	N/A	N/A
Compound 1	111.4 $\pm$ 5.6		1	5.9 $\pm$ 0.3	
Compound 2	110.1 $\pm$ 5.9	0.99	0.9	5.8 $\pm$ 0.1	0.99
SKF96365	110.0 $\pm$ 7.2	0.99	0.9	5.1 $\pm$ 0.3	0.13
Nifedipine	98.8 $\pm$ 4.7	0.41	0.8	7.1 $\pm$ 0.2** <sup>a</sup>	0.02
Pyr3	78.1 $\pm$ 7.2** <sup>a</sup>	0.002	0.7	6.4 $\pm$ 0.3	0.64
HC-070	99.1 $\pm$ 3.3	0.43	0.8	6.2 $\pm$ 0.3	0.89

<sup>a</sup> One-way ANOVA followed by Dunnett's multiple comparison test  $p$ -values < 0.05 were expressed as \*,  $p$ -values < 0.01 were expressed as \*\*, and  $p$ -values < 0.0001 were expressed as \*\*\* vs compound 1.

<sup>b</sup>  $E_{\max}$  of each calcium channel inhibitor was expressed relative to the corresponding  $E_{\max}$  of compound 1 and presented as the relative  $E_{\max}$ .

### 3.3. Compound 1-induced relaxation is endothelium- and NO-independent

The removal of endothelium did not seem to affect the maximal relaxation effect of compound 1 ( $E$ ,  $E_{\max}$  117.4  $\pm$  12.7%,  $pEC_{50}$  5.4  $\pm$  0.2,  $n = 7$ ) when compared to endothelium intact aortic rings ( $E +$ ,  $E_{\max}$  119.8  $\pm$  4.9%,  $pEC_{50}$  5.3  $\pm$  0.1,  $n = 7$ ). When in combination with L-NAME, the endothelium-denuded aortic tissues relaxed at a similar magnitude to the control ( $E_{\max}$  106.4  $\pm$  1.9%,  $pEC_{50}$  5.4  $\pm$  0.1,  $n = 4$ ) (Fig. 3a).

To further investigate whether compound 1 is involved in NO-mediated response, SNP was employed. Incubation with compound 1 (30  $\mu$ M) did not seem to affect the SNP-induced relaxation in the aorta. The magnitude of response to SNP was similar between the control group ( $p = 0.1$ ) ( $E_{\max}$  120.8  $\pm$  4.5%,  $pEC_{50}$  8.4  $\pm$  0.1,  $n = 6$ ) and compound 1 treated group ( $E_{\max}$  105.3  $\pm$  5.6%,  $pEC_{50}$  8.7  $\pm$  0.1,  $n = 6$ ) (Fig. 3b).

### 3.4. Compound 1-induced relaxation does not involve adrenergic receptors, cyclic nucleotides and potassium channels

When treated with  $\alpha$ -adrenergic receptor antagonists, rauwolscine and prazosin, the relaxation response to compound 1 was not affected compared to the control (Fig. 4a, Table 2). Similarly, treatment with  $\beta$ -adrenergic receptor antagonists, timolol and propranolol, also did not

affect the relaxation of compound 1 in response to phenylephrine-induced contraction (Fig. 4b, Table 2).

In order to investigate the effects of phosphodiesterase inhibitors on compound 1-induced relaxation, IBMX was used. Pre-treatment with IBMX did not alter the relaxation curve of compound 1 in aortic rings pre-contracted with phenylephrine (Fig. 4c, Table 2).

The next experiment assessed whether potassium channels were involved in compound 1-induced relaxation. The aortic rings were pre-incubated with a potassium channel blocker, TEA or 4-AP, before inducing contraction with phenylephrine. The rings pre-incubated with TEA were not influenced by compound 1 when compared to the control. Pre-incubation with 4-AP also did not affect the maximal response and potency of 1 (Fig. 4d, Table 2).

### 3.5. Compound 1-induced relaxation mechanism may involve other channels than L / T-type $Ca^{2+}$ channels

In the first set of experiments, the aortic rings were pre-incubated with nifedipine prior to performing the 1 concentration-response curve. Pre-treatment with nifedipine did not seem to affect 1-induced relaxation on aortic rings pre-contracted with PE with  $E_{\max}$  values of (control = 119.8  $\pm$  4.9%, nifedipine treated = 128.8  $\pm$  6.7%;  $p = 0.3$ ) (Fig. 5a). In terms of potency no significant difference was observed between control and nifedipine treated group, with  $pEC_{50}$  values of: (control = 5.7  $\pm$  0.4, nifedipine treated = 5.7  $\pm$  0.1;  $p = 0.98$ ).

To further study the involvement of L-type  $Ca^{2+}$  channels in 1-induced relaxation, a different experimental protocol involving pre-incubation with nifedipine and a single addition of 1 on PE-induced contraction was performed. Aortic rings treated with DMSO (0.22%) served as vehicle control. The PE tone was rapidly reduced after 10 min of addition to 3.5  $\pm$  0.8 mN ( $p = 0.0017$ ), while the addition of vehicle did not significantly affect the PE-induced contraction (8.1  $\pm$  1.4 mN;  $p = 0.22$ ) (Fig. 5b).

The next step of the experiment was to examine the involvement of T-type  $Ca^{2+}$  channels. In the first set of experiments, the aortic rings were pre-incubated with verapamil prior to performing the compound 1 concentration-response curve. Pre-treatment with verapamil did not seem to affect compound 1-induced relaxation on aortic rings pre-contracted with PE with the maximal response (control = 119.3  $\pm$  4.4%, verapamil treated = 120.5  $\pm$  7.8%;  $p = 0.9$ ) (Fig. 6a). In terms of potency no significant difference was observed between control and verapamil treated group, with  $pEC_{50}$  values of: (control = 5.2  $\pm$  0.2, verapamil treated = 5.0  $\pm$  0.01;  $p = 0.2$ ).

To further study the involvement of T-type  $Ca^{2+}$  channels in compound 1-induced relaxation, a different experimental protocol involving pre-incubation with verapamil and a single addition of compound 1 on

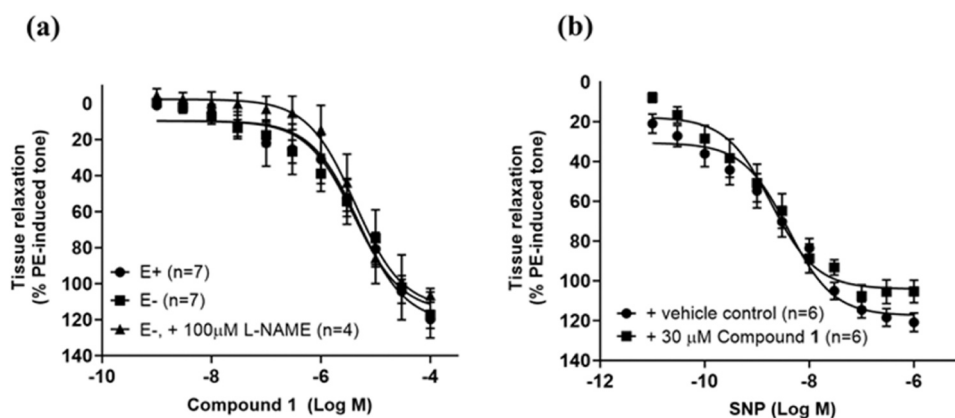


**Fig. 3.** Effects of (a) endothelium removal (E-) and in combination with L-NAME (E- + L-NAME) on compound 1-induced relaxation (b) 1 incubation on SNP-induced relaxation. Tissue relaxations were expressed as the percentage of phenylephrine-induced contraction. Data are presented as mean values  $\pm$  SEM of  $n$  number of animals. PE, phenylephrine.

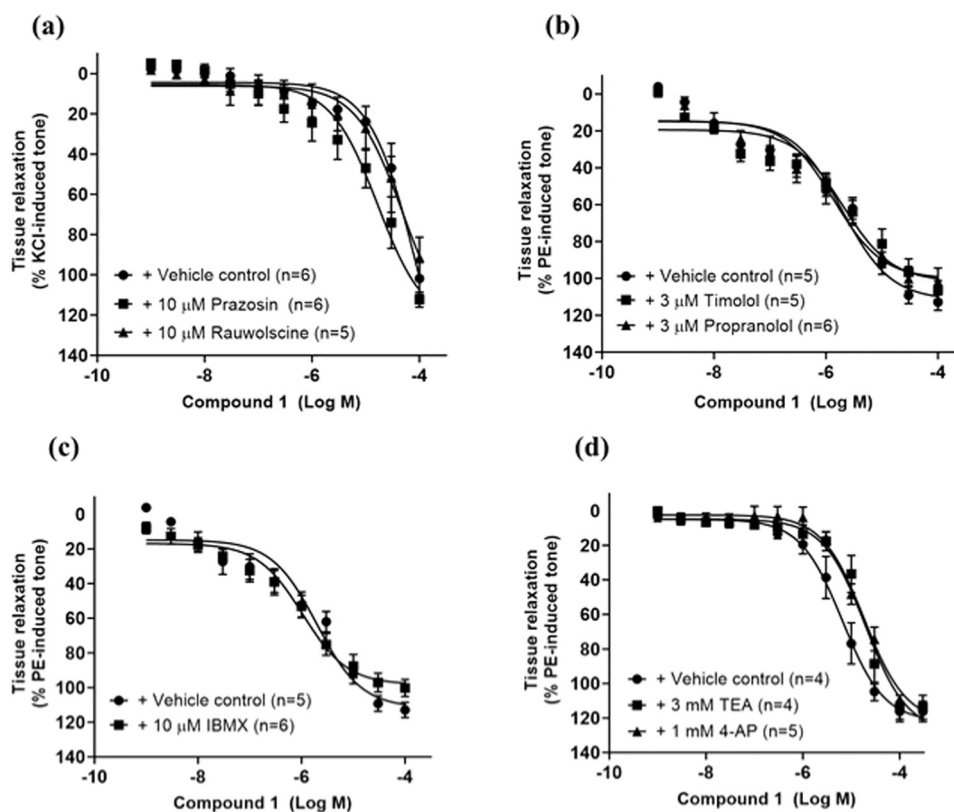


**Fig. 4.** Effects of (a)  $\alpha$ -adrenergic receptor antagonists (prazosin and rauwolscine, 10  $\mu$ M) (b)  $\beta$ -adrenergic antagonists (timolol and propranolol, 3  $\mu$ M) (c) phosphodiesterase inhibitor, (IBMX, 1  $\mu$ M) (d) potassium channel blockers (TEA, 3 mM and 4-AP, 1 mM) on compound 1-induced relaxation. Tissue relaxations were expressed as the percentage of respective KCl- and phenylephrine-induced contraction. Data are presented as mean values  $\pm$  SEM of  $n$  number of animals. PE, phenylephrine, KCl, potassium chloride, IBMX, isobutylmethylxanthine, TEA, tetraethylammonium chloride, 4-AP, 4-aminopyridine.

**Table 2**

Summary of the  $E_{max}$  and  $pEC_{50}$  of compound 1-induced relaxation when pre-treated with  $\alpha$ -adrenergic antagonists (prazosin and rauwolscine, 10  $\mu$ M),  $\beta$ -adrenergic antagonists (propranolol and timolol, 3  $\mu$ M), a PDE inhibitor, (IBMX, 1  $\mu$ M), and potassium channel blockers (TEA, 3 mM and 4-AP, 1 mM). The values are the mean  $\pm$  SEM of  $n$  number of animals.

	$E_{max}$ (%)	$p$ -value	$pEC_{50}$	$p$ -value
Vehicle control	101.8 $\pm$ 7.8		4.0 $\pm$ 0.1	
Prazosin	112.2 $\pm$ 3.6 <sup>a</sup>	0.49	4.7 $\pm$ 0.1 <sup>a</sup>	0.80
Rauwolscine	91.3 $\pm$ 9.9 <sup>a</sup>	0.52	4.3 $\pm$ 0.2 <sup>a</sup>	0.96
Vehicle control	112.9 $\pm$ 4.3		5.7 $\pm$ 0.5	
Propranolol	101.7 $\pm$ 7.3 <sup>a</sup>	0.32	5.8 $\pm$ 0.4 <sup>a</sup>	0.97
Timolol	106.3 $\pm$ 5.0 <sup>a</sup>	0.67	5.7 $\pm$ 0.2 <sup>a</sup>	0.77
Vehicle control	112.9 $\pm$ 4.3		5.7 $\pm$ 0.1	
IBMX	100.2 $\pm$ 4.9 <sup>a</sup>	0.09	5.9 $\pm$ 0.1 <sup>b</sup>	0.26
Vehicle control	116.1 $\pm$ 5.8		5.1 $\pm$ 0.2	
TEA	113.7 $\pm$ 6.8 <sup>a</sup>	0.91	4.7 $\pm$ 0.1 <sup>a</sup>	0.07
4-AP	111.9 $\pm$ 1.9 <sup>a</sup>	0.76	4.7 $\pm$ 0.1 <sup>a</sup>	0.06

<sup>a</sup> One-way ANOVA followed by Dunnett's multiple comparison test,  $p < 0.05$ .

<sup>b</sup> Student's unpaired t-test,  $p < 0.05$ .

PE-induced contraction was performed. PE-induced contraction prior to verapamil incubation was  $11.8 \pm 0.7$  mN. However, upon incubation with verapamil, the PE contraction was reduced to  $6.7 \pm 0.3$  mN ( $p = 0.0008$ ). Thereafter, compound 1 or vehicle was added to the same tissue. Addition of vehicle (control) reduced PE contraction to  $4.8 \pm 1.0$  mN ( $p = 0.03$ ), while the addition of 1 reduced the PE contraction rapidly after 10 min of addition to ( $1.8 \pm 0.5$  mN;  $p < 0.0001$ ) (Fig. 6b).

### 3.6. Compound 1 inhibits extracellular $Ca^{2+}$ -induced contraction with no effect on intracellular stored calcium

The contractile response to  $CaCl_2$  following pre-treatment with compound 1 (10 and 30  $\mu$ M) was concentration-dependent, with complete abolishment observed in the presence of 30  $\mu$ M compound 1. Nifedipine, however, elicited a contraction of  $48.8 \pm 9.8\%$  ( $n = 6$ ) (Fig. 7a).

When compound 1 was tested for its role on intracellular stored calcium, compound 1 did not affect phenylephrine-induced contraction ( $p = 0.45$ ) in  $Ca^{2+}$ -free Krebs solution (control,  $E_{max}$  25.6  $\pm$  4.0%; 1,  $E_{max}$  21.3  $\pm$  3.8%) (Fig. 7b).

### 3.7. Compound 1 inhibits TRPC3, TRPC4, TRPC5 and TRPC6 channels

To assess the effect of 1 on TRPC3 and TRPC6 channels, HEK T-REX cells overexpressing TRPC3 and HEK-293 transiently expressing TRPC6 were pre-incubated with 1 before activation with OAG. Compound 1 concentration-dependently suppressed activation of  $Ca^{2+}$  influx mediated by OAG. For TRPC3, the largest effect was observed at 30  $\mu$ M and 100  $\mu$ M of compound 1 and with a  $pIC_{50}$  value of 5.2 ( $IC_{50}$  6  $\mu$ M) (Fig. 8a, b). Similarly, for TRPC6 full inhibition of the OAG response was seen at 30 and 100  $\mu$ M with a slight response at 10  $\mu$ M of compound 1, with a  $pIC_{50}$  value of 5.3 ( $IC_{50}$  5  $\mu$ M) (Fig. 8c, d). These data suggest that compound 1 is able to inhibit both TRPC3:C3 and TRPC6:C6 channels with similar potency.

The effects of compound 1 on TRPC4 and TRPC5 channel activity were tested on hTRPC4 or hTRPC5-overexpressing (Tet+) HEK T-REX™ cells. In order to compare the effects on vascular relaxation and TRPC channel modulation by compound 1, we used a physiologically relevant TRPC4/5 activator S1P for the assays, which does not induce significant

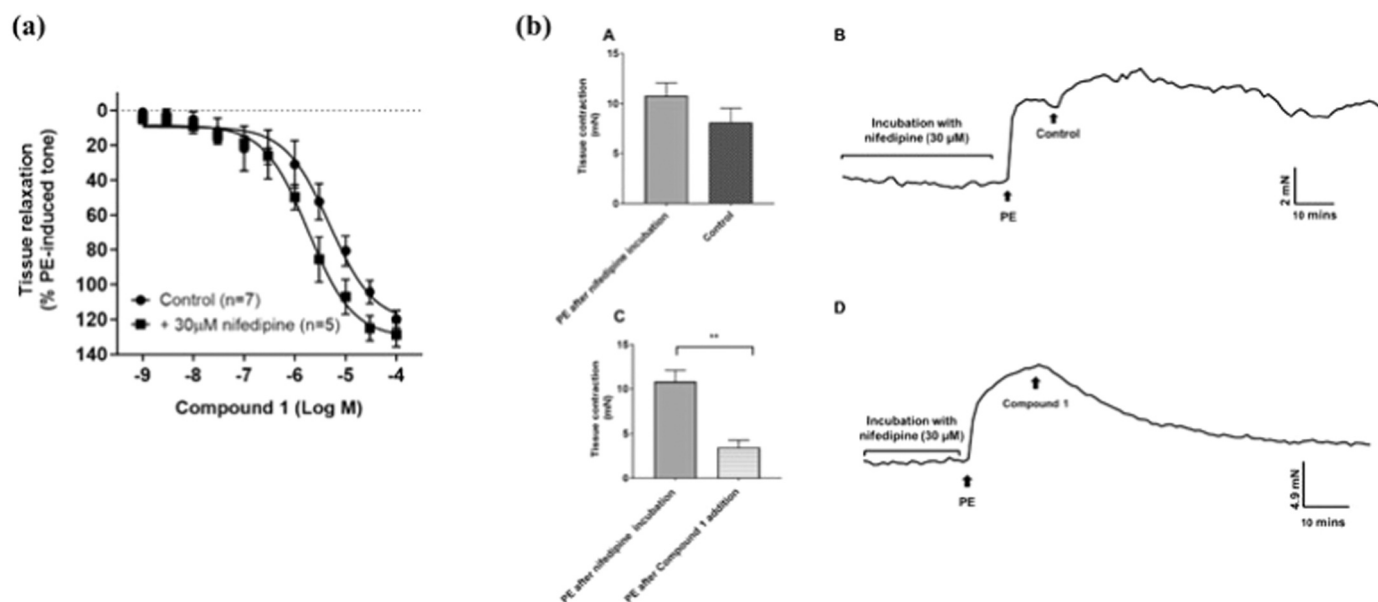


**Fig. 5.** (a) Effects of nifedipine on compound 1 concentration-response curve on rat aortae. Tissue responses have been expressed as a percentage of PE-induced contraction and are shown as means  $\pm$  SEM of 5–7 animals (b) Effect of pre-incubation with nifedipine (30  $\mu$ M) followed by addition of A) vehicle control B) compound 1 (30  $\mu$ M) on PE-induced contractions. Representative trace recordings of the effect of pre-incubation with nifedipine (30  $\mu$ M) followed by the addition of C) vehicle control D) compound 1 (30  $\mu$ M) on PE-induced contractions. Tissue responses have been expressed as a force of contraction in force mN and are shown as means  $\pm$  SEM of 5–6 animals. (paired t-test: \*  $p < 0.05$ , \*\*\*  $p < 0.001$ ). (Abbreviations: PE = phenylephrine; mN = milliNewton; mins = minutes).

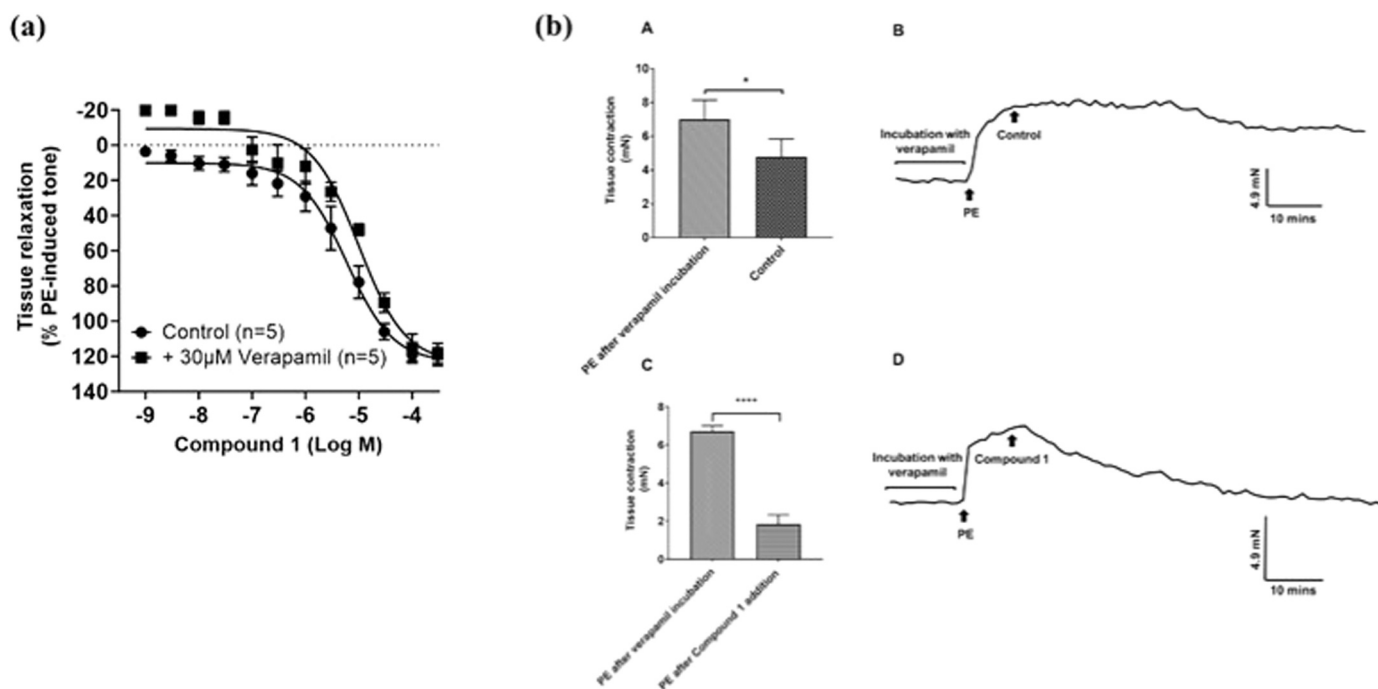


**Fig. 6.** (a) Effects of verapamil against compound 1 concentration-response curve on rat aortae. Tissue responses have been expressed as a percentage of PE-induced contraction and are shown as means  $\pm$  SEM of 5 animals (b) Effect of pre-incubation with verapamil (30  $\mu$ M) followed by addition of A) vehicle (control) B) compound 1 (30  $\mu$ M) on PE-induced contractions. Representative trace recordings of the effect of pre-incubation with verapamil (30  $\mu$ M) followed by the addition of C) vehicle (control) D) 1 (30  $\mu$ M) on PE-induced contractions. Tissue responses have been expressed as a force of contraction in force mN and are shown as means  $\pm$  SEM of 5–6 animals. (paired t-test: \*  $p < 0.05$ , \*\*\*\*  $p < 0.0001$ ). (Abbreviations: PE = phenylephrine; mN = milliNewton; mins = minutes).

Ca<sup>2+</sup> influx in wild-type HEK-293 cells (Zhu et al., 2019). Compound 1 inhibited S1P-evoked Ca<sup>2+</sup> influx mediated by hTRPC4 and hTRPC5 (Fig. 8e, g), with a pIC<sub>50</sub> value of 5.7 (IC<sub>50</sub> 2  $\mu$ M) (Fig. 8f, h). Similar to TRPC3 and TRPC6 channels, full inhibition of TRPC4 and TRPC5 channels was observed at 30 and 100  $\mu$ M of compound 1. These data show that compound 1 at higher concentration is able to inhibit all the

TPRC channels but with slightly higher potency at TRPC4 and TRPC5 channels.

#### 4. Discussion

Our previous research uncovered that compound 2 (schwarzizincine

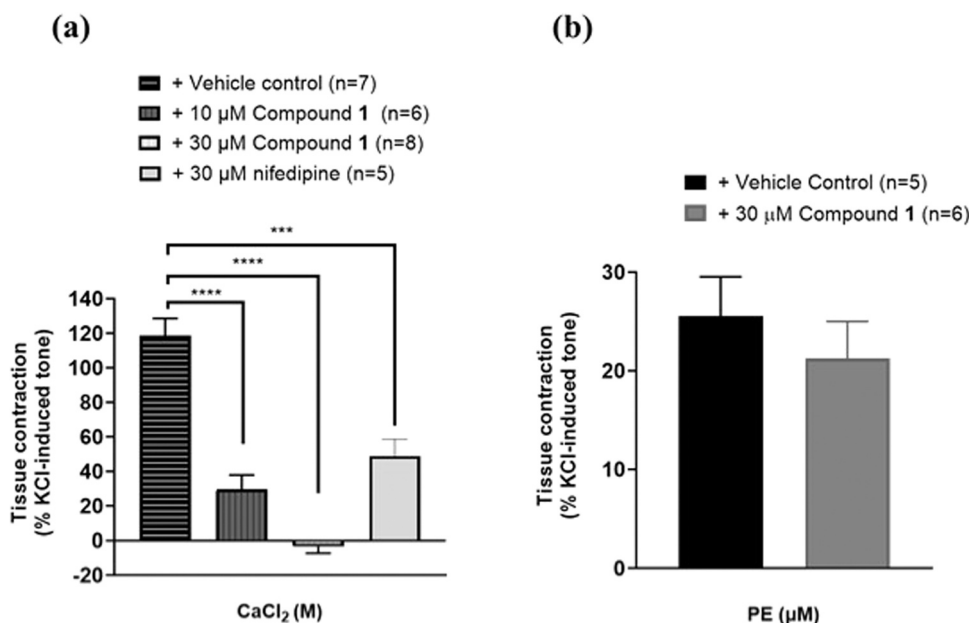


Fig. 7. Effects of (a) compound 1 and nifedipine on  $\text{CaCl}_2$ -induced contraction in calcium free-Krebs. The maximum contraction measured in the vehicle control segments was  $118.7 \pm 9.9\%$  ( $n = 7$ ), compound 1 ( $10 \mu\text{M}$ ) =  $29.5 \pm 8.4\%$  ( $n = 6$ ), and  $0\%$  treated with compound 1 ( $30 \mu\text{M}$ ) (b) vehicle control and compound 1 ( $30 \mu\text{M}$ ) on the maximal contractile response of phenylephrine ( $10 \mu\text{M}$ ) in  $\text{Ca}^{2+}$ -free Krebs-Ringer solution. Data are presented as mean values  $\pm$  SEM of  $n$  number of animals. KCl, potassium chloride,  $\text{CaCl}_2$ , calcium chloride.

A) exerts a relaxation effect on vascular smooth muscle, and this effect was not influenced by the chirality at C-2 (Krishnan et al., 2020; Mak et al., 2022; Lee et al., 2022). As with compound 2, the chirality in compound 1 is assumed to have no impact on its relaxation effect. Given our limited knowledge of compound 1, we adopted a stepwise basic pharmacological approach to lay a foundation for further exploration and gain a better understanding of its vascular effect.

The vasorelaxant activity of compound 1 against rat aortae was compared with four types of calcium channel blockers: an L-type calcium channel blocker (nifedipine), a non-selective TRPC channel inhibitor (SKF96365), a TRPC3 channel-selective inhibitor (Pyr3) and a TRPC3/4/5 channel inhibitor (HC-070) (Just et al., 2018; Mak et al., 2022). Compound 1 exhibited relaxation properties comparable to those of its parent compound 2 and SKF96365, with similar  $\text{pEC}_{50}$  and  $E_{\text{max}}$  values.

Although compound 1 exhibited similar  $E_{\text{max}}$  values as nifedipine, it was approximately 25-fold less potent than nifedipine. Pyr3, on the other hand, displayed the lowest relaxation response among all the calcium channel inhibitors examined. Notably, Pyr3 exhibited the same  $\text{IC}_{50}$  value for both Orai and TRPC3 channels ( $0.54 \mu\text{M}$ ), which could account for its reduced efficacy as a calcium channel inhibitor. Future investigations utilising more potent TRPC3 inhibitors hold the potential to provide a more nuanced understanding of the specific role of TRPC3 in calcium signalling. The concentration-dependent reduction in vascular tone observed for both Pyr3 and HC-070 indicates that TRPC3, TRPC4, and TRPC5 channels in the rat aorta are vital in controlling aortic contractility. Collectively, the rank of vasorelaxant response ( $E_{\text{max}}$ ) for these compounds is: compound 2 = 1 = SKF96365  $\geq$  HC-070 = Nifedipine > Pyr3.

The  $\alpha$ - and  $\beta$ -adrenergic receptors signalling pathway is one of the major pathways in mediating vascular activity.  $\alpha$ -adrenergic receptors are responsible for vasoconstriction, while  $\beta$ -adrenergic receptors are involved in vasodilation. Therefore, blockade of the  $\alpha$ -adrenergic receptor would lead to relaxation. The relevance of investigating  $\alpha$ - and  $\beta$ -adrenergic receptors is supported by current findings that 1 reduces phenylephrine-induced contraction. However, this possibility was ruled out as no influence of  $\alpha$ -adrenergic (rauwolscine and prazosin) and  $\beta$ -adrenergic (timolol and propranolol) receptor antagonists were

observed on 1-induced relaxation. These results indicate that 1 does not act directly on  $\alpha$ - and  $\beta$ -adrenergic receptors.

The endothelium forms an integral part of the vasculature and releases various vasodilatory factors, including nitric oxide (NO), prostacyclin ( $\text{PGI}_2$ ), and endothelium-derived hyperpolarising factors (EDHFs). TRPC3, TRPC4, and TRPC6 channels are found in the vascular endothelium of some blood vessels, including the thoracic aortae of rats (Freichel et al., 2001; Liang et al., 2018; Senadheera et al., 2012). TRPC3, in particular, has been proposed in earlier studies to be involved in the feedback mechanism controlling NO production on the endothelium, leading to smooth muscle relaxation (Grayson et al., 2017). On the other hand, studies on endothelial cells from TRPC4<sup>-/-</sup> mice lack a highly  $\text{Ca}^{2+}$ -permeable, store-dependent current, supporting the role of TRPC4 in endothelium-mediated vasorelaxations (Tiruppathi et al., 2002). However, our present findings demonstrate that 1-induced relaxation is dependent neither on endothelium nor nitric oxide relaxation pathway. This rules out the possible influence of endothelium on 1-induced relaxation in the aorta.

Secondary messengers, i.e., cyclic nucleotides (cAMP and cGMP), play a central role in mediating the relaxation of vascular tissues. TRPC3 is inhibited by direct phosphorylation via cGMP/protein kinase G (Chen et al., 2009; Kwan et al., 2004) and protein kinase C (Albert and Large, 2004; Trebak et al., 2005). Therefore, further experiments were carried out to verify the possible role of secondary messengers in compound 1-induced relaxation. As cyclic nucleotides are metabolised by phosphodiesterases (PDEs), the inhibition of PDEs is assumed to retain the amount of active cAMP/protein kinase A or cGMP/protein kinase G, leading to enhanced and sustained relaxation of the vasculature. However, pre-treatment with IBMX, a non-selective phosphodiesterase inhibitor, did not affect compound 1-induced relaxation. This finding shows that compound 1 does not modulate or affect any of the nucleotide-induced vascular relaxations. Our finding further corroborates a previous study on TRPC3 knockout mice. There was no clear link between TRPC3 function and cGMP- or protein kinase G-induced relaxation of the aorta or hind limb circulation (Loga et al., 2013).

The interplay between TRPC channels and potassium channels, particularly  $\text{K}_{\text{Ca}}$  channels that open in response to  $\text{Ca}^{2+}$ , has been well-established in smooth muscle cell depolarisation and vasoconstriction

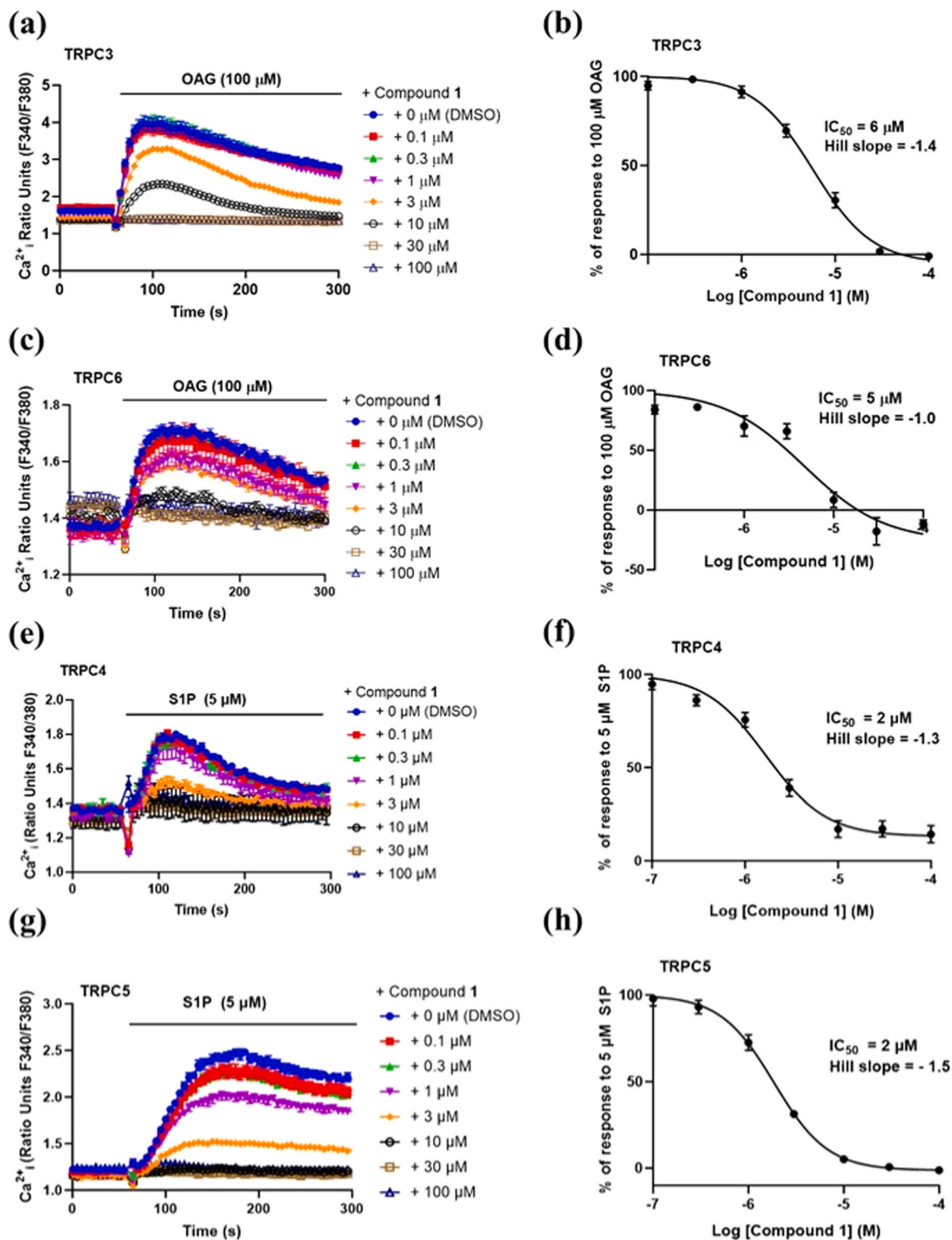


**Fig. 8.** Representative  $[Ca^{2+}]_i$  measurements from a single 96-well plate ( $N = 6$ ), showing  $Ca^{2+}$  inhibition by 0.1–100  $\mu M$  compound 1 in the presence of 100  $\mu M$  OAG in (a) (Tet+) HEK T-REx<sup>TM</sup> cells expressing hTRPC3 or (c) HEK WT cells expressing hTRPC6 or in the presence of S1P-mediated  $Ca^{2+}$  influx in (e) HEK T-REx<sup>TM</sup> cells overexpressing hTRPC4 and (g) HEK T-REx<sup>TM</sup> overexpressing hTRPC5. (b, d, f, h) Concentration-response curve to compound 1 for experiments in (a), (c), (e), and (g), respectively. Responses were calculated at 90 – 140 s (A-D; hTRPC3/6), 110 – 130 s (E/F; hTRPC4) or 150 – 180 s (G/H; hTRPC5) compared to baseline  $[Ca^{2+}]_i$  at 0 – 55 s. Data are shown as mean responses  $\pm$  SEM (hTRPC3:  $n/N = 5/30$ ; hTRPC6:  $n/N = 5/30$ ; hTRPC4:  $n/N = 5/30$ ; hTRPC5:  $n/N = 5/30$ ).

(Behringer and Hakim, 2019). In previous studies, stimulation of  $\alpha_1$ -adrenergic receptors has been shown to involve potassium conductance in rat aortic smooth muscle (Tammaro et al., 2004). Our data show no evidence of potassium channels in regulating TRPC3/6.

Pre-incubation with nifedipine or verapamil did not appear to

influence compound 1 concentration-dependent relaxation. However, in separate experiments, the combined treatment of compound 1 and nifedipine or verapamil significantly decreased PE contraction. These observations suggest that the inhibitory effects of compound 1, nifedipine and verapamil on PE contraction exhibit different mechanisms

whereby compound **1** may not directly affect L- or T-type  $\text{Ca}^{2+}$  channels in rat aorta.

In addition to investigating the effect of compound **1** on  $\text{Ca}^{2+}$  influx, we also examined its effect on intracellular  $\text{Ca}^{2+}$  levels, as the mobilisation of  $[\text{Ca}^{2+}]_i$  is controlled by  $\text{Ca}^{2+}$  influx and intracellular store activation. Our results showed that pre-treatment with compound **1** did not alter the contraction of aortic rings induced by phenylephrine in  $\text{Ca}^{2+}$ -free Krebs buffer. This suggests that the attenuation of PE-induced contractions by compound **1** is due to the inhibition of extracellular  $\text{Ca}^{2+}$  influx and not the modulation of phasic contraction in the absence of extracellular  $\text{Ca}^{2+}$ . The phasic component is typically linked to inositol triphosphate (InsP3)-evoked release of  $\text{Ca}^{2+}$  from the sarcoplasmic reticulum (SR) store.

Considering that the relaxation effect of compound **1** is further enhanced in the presence of verapamil or nifedipine, which suggests the involvement of mechanisms beyond L/T-type  $\text{Ca}^{2+}$  channels, it is intriguing to speculate that compound **1** blocks extracellular  $\text{Ca}^{2+}$  entry via TRPC channels. Additionally, several lines of evidence derived from animal models and human subjects highlight the involvement of TRPC in VSMC. TRPC3 and TRPC6 mRNA and protein expression have been demonstrated in VSMCs from different vascular beds (Alonso-Carbajo et al., 2017). However, the involvement of TRPC4 channels in vascular physiology is not yet well-defined, while TRPC5 expression is much lower than the other TRPC channels in VSMC (Alonso-Carbajo et al., 2017; Okada et al., 1998; Philipp et al., 1998). This is in accordance with our previous laboratory findings that the role of the TRPC3 channel appears to be dominant in vascular relaxation compared to that of TRPC4 and TRPC5 channels, as no relaxation effect was observed at nanomolar concentrations of HC-070, a well-characterised TRPC4/5 channel-selective inhibitor (Mak et al., 2022).

To confirm any possible modulatory effect of compound **1** on TRPC channels, we carried out  $[\text{Ca}^{2+}]_i$  measurements using HEK-293 cells overexpressing human TRPC3/4/5/6 to monitor calcium dynamics. Compound **1** inhibits  $\text{Ca}^{2+}$  influx through homomeric hTRPC3, 4, 5, and 6 channels at low micromolar range ( $\text{IC}_{50}$  of 6, 2, 2 and 5  $\mu\text{M}$ , respectively). The  $\text{pIC}_{50}$  of compound **1** measured at TRPC3, and TRPC6 was similar to other less selective small compounds such as SKF96365 (TRPC6,  $\text{pIC}_{50}$  5.4) (Inoue et al., 2001) and Pyr10 (TRPC3, 6.1) (Schleifer et al., 2012). These findings are further supported by the results of the rat aorta functional assay, which yielded a  $\text{pEC}_{50}$  of 5.7.

In vivo testing of compound **1** was carried out on *Caenorhabditis elegans*, to observe possible toxicity and physiological responses of the worm. Long-term exposure to compound **1** did not affect the worm's life span but reduced their pharyngeal pumping activity, a physiological response that is mediated by calcium movement (Bargmann, 1998; Lee et al., 1997; Steger et al., 2005) (Supplementary data, Fig. S3 and Fig. S4). This additional evidence supports compound **1** as a possible inhibitor of calcium dynamics in the physiological regulation of a native system. It is worth mentioning that our study has certain limitations that should be taken into account. Specifically, we did not test the effects of compound **1** on other TRP channels, such as TPRV. While this was a deliberate decision based on the research focus, further research should address the effects of compound **1** on these channels. Further experiments, such as patch-clamp electrophysiology experiments, photo-affinity labelling, and molecular modelling studies, would be required to confirm the mechanistic involvement of TRPC channels in compound **1**'s inhibitory effects.

## 5. Conclusion

In conclusion, our study reveals that *N*-Phenethyl-1-phenyl-pentan-3-amine (**1**) exhibits a vasorelaxant effect similar to its natural parent compound, schwartzincine A (**2**), highlighting its potential as a calcium-modulating compound. The evidence we have to date shows that the inhibitory effect of compound **1** is endothelium- and NO-independent, and part of the compound **1**-induced relaxation involves non-selective

inhibition of extracellular  $\text{Ca}^{2+}$  influx, including multiple TRPC channels.

## Ethics approval

University of Nottingham's Animal Welfare and Ethics Review Body approved the experimental protocol (UNMC12).

## CRediT authorship contribution statement

KG: Investigation, Data curation, Writing – original draft. YYM: Investigation, Data curation, Writing – review & editing. FKL: Investigation, Data curation. KNT and KHL: Conceptualization, Supervision, Project administration, Writing – review & editing, Funding acquisition. CK and SMT: Supervision, Writing – review & editing. CCB and RSB: Data analysis, Writing – review & editing, Funding acquisition.

## Declaration of Competing Interest

There is no conflict of interest.

## Data Availability

Data will be made available on request.

## Acknowledgements

This study is supported by Malaysia Toray Science Foundation (Grant No. TML-CA/17.195(17/G62), grants awarded by the Ministry of Higher Education Malaysia (Grant No. FRGS/1/2017/STG01/UNIM/02/3 and FRGS/1/2017/SKK10/UNIM/01/1) and the Schachter award from the British Pharmacological Society. TRPC channel studies performed at the University of Leeds were supported by the British Heart Foundation (BHF; PG/19/2/34084).

## Appendix A. Supporting information

Supplementary data associated with this article can be found in the online version at doi:10.1016/j.phytol.2023.11.007.

## References

- Abramowitz, J., Birnbaumer, L., 2009. Physiology and pathophysiology of canonical transient receptor potential channels. *Faseb J.* 23 (2), 297–328. <https://doi.org/10.1096/fj.08-119495>.
- Akbulut, Y., Gaunt, H.J., Muraki, K., Ludlow, M.J., Amer, M.S., Bruns, A., Vasudev, N.S., Radtke, L., Willot, M., Hahn, S., Seitz, T., Ziegler, S., Christmann, M., Beech, D.J., Waldmann, H., 2015. (-)-EnglerinA is a potent and selective activator of TRPC4 and TRPC5 calcium channels. *Angew. Chem. Int. Ed. Engl.* 54 (12), 3787–3791. <https://doi.org/10.1002/anie.201411511>.
- Albert, A.P., Large, W.A., 2004. Inhibitory regulation of constitutive transient receptor potential-like cation channels in rabbit ear artery myocytes. *J. Physiol.* 560 (1), 169–180. <https://doi.org/10.1113/jphysiol.2004.071738>.
- Alonso-Carbajo, L., Kecskes, M., Jacobs, G., Pironet, A., Syam, N., Talavera, K., Vennekens, R., 2017. Muscling in on TRP channels in vascular smooth muscle cells and cardiomyocytes. *Cell Calcium* 66, 48–61. <https://doi.org/10.1016/j.ceca.2017.06.004>.
- Álvarez-Miguel, I., Ciudad, P., Pérez-García, M.T., López-López, J.R., 2017. Differences in TRPC3 and TRPC6 channels assembly in mesenteric vascular smooth muscle cells in essential hypertension. *J. Physiol.* 595 (5), 1497–1513. <https://doi.org/10.1113/jp273327>.
- Arsyad, A., Dobson, G.P., 2016. Lidocaine relaxation in isolated rat aortic rings is enhanced by endothelial removal: possible role of Kv, KATP channels and A2a receptor crosstalk. *BMC Anesthesiol.* 16 (1), 121 <https://doi.org/10.1186/s12871-016-0286-y>.
- Bargmann, C.I., 1998. Neurobiology of the *Caenorhabditis elegans* genome. *Science* 282 (5396), 2028–2033. <https://doi.org/10.1126/science.282.5396.2028>.
- Behringer, E.J., Hakim, M.A., 2019. Functional Interaction among K(Ca) and TRP Channels for Cardiovascular Physiology: Modern Perspectives on Aging and Chronic Disease. *Int. J. Mol. Sci.* 20 (6), 1380. <https://doi.org/10.3390/ijms20061380>.
- Bergson, P., Lipkind, G., Lee, S.P., Duban, M.E., Hanck, D.A., 2011. Verapamil block of T-type calcium channels. *Mol. Pharm.* 79 (3), 411–419. <https://doi.org/10.1124/mol.110.069492>.

- Bon, R.S., Wright, D.J., Beech, D.J., Sukumar, P., 2022. Pharmacology of TRPC Channels and Its Potential in Cardiovascular and Metabolic Medicine. *Annu Rev. Pharm. Toxicol.* 62, 427–446. <https://doi.org/10.1146/annurev-pharmtox-030121-122314>.
- Chen, J., Crossland, R.F., Noorani, M.M., Marrelli, S.P., 2009. Inhibition of TRPC1/TRPC3 by PKG contributes to NO-mediated vasorelaxation. *Am. J. Physiol. Heart Circ. Physiol.* 297 (1), H417–H424. <https://doi.org/10.1152/ajpheart.01130.2008>.
- Chen, X., Yang, D., Ma, S., He, H., Luo, Z., Feng, X., Cao, T., Ma, L., Yan, Z., Liu, D., Tepel, M., Zhu, Z., 2010. Increased rhythmicity in hypertensive arterial smooth muscle is linked to transient receptor potential canonical channels. *J. Cell Mol. Med* 14 (10), 2483–2494. <https://doi.org/10.1111/j.1582-4934.2009.00890.x>.
- Dietrich, A., Mederos y Schnitzler, M., Kalwa, H., Storch, U., Gudermann, T., 2005. Functional characterisation and physiological relevance of the TRPC3/6/7 subfamily of cation channels. *Naunyn Schmiede Arch. Pharm.* 371 (4), 257–265. <https://doi.org/10.1007/s00210-005-1052-8>.
- Earley, S., Brayden, J.E., 2015. Transient receptor potential channels in the vasculature. *Physiol. Rev.* 95 (2), 645–690. <https://doi.org/10.1152/physrev.00026.2014>.
- Facemire, C.S., Mohler, P.J., Arendshorst, W.J., 2004. Expression and relative abundance of short transient receptor potential channels in the rat renal microcirculation. *Am. J. Physiol. Ren. Physiol.* 286 (3), F546–F551. <https://doi.org/10.1152/ajprenal.00338.2003>.
- Freichel, M., Suh, S.H., Pfeifer, A., Schweig, U., Trost, C., Weissgerber, P., Biel, M., Philipp, S., Freise, D., Droogmans, G., Hofmann, F., Flockerzi, V., Nilius, B., 2001. Lack of an endothelial store-operated Ca<sup>2+</sup> current impairs agonist-dependent vasorelaxation in TRP4<sup>-/-</sup> mice. *Nat. Cell Biol.* 3 (2), 121–127. <https://doi.org/10.1038/35055019>.
- Gokce, G., Arun, M.Z., 2014. Ergothioneine produces relaxation in isolated rat aorta by inactivating superoxide anion. *Eur. Rev. Med Pharm. Sci.* 18 (21), 3339–3345.
- Grayson, T.H., Murphy, T.V., Sandow, S.L., 2017. Transient receptor potential canonical type 3 channels: Interactions, role and relevance - A vascular focus. *Pharmacol. Ther.* 174, 79–96. <https://doi.org/10.1016/j.pharmthera.2017.02.022>.
- Guan, Y.Y., Kwan, C.Y., Daniel, E.E., 1988. The effects of EGTA on vascular smooth muscle contractility in calcium-free medium. *Can. J. Physiol. Pharm.* 66 (8), 1053–1056. <https://doi.org/10.1139/y88-172>.
- Huang, P.-Q., Wang, Y., Xiao, K.-J., Huang, Y.-H., 2015. A general method for the direct transformation of common tertiary amides into ketones and amines by addition of Grignard reagents. *Tetrahedron* 71 (24), 4248–4254. <https://doi.org/10.1016/j.tet.2015.04.074>.
- Idris, B., Asmawi, M.Z., Nasiba, U.S., Mahmud, R., & Abubakar, K. (2015). Antihypertensive and Vasorelaxant Effect of *Alstonia scholaris* Stem Bark Extracts and Fractions. In (pp. 327–334). *Int. J. Pharmacol.*
- Inoue, R., Okada, T., Onoue, H., Hara, Y., Shimizu, S., Naitoh, S., Ito, Y., Mori, Y., 2001. The transient receptor potential homologue TRP6 is the essential component of vascular alpha(1)-adrenoceptor-activated Ca(2+)-permeable cation channel. *Circ. Res* 88 (3), 325–332. <https://doi.org/10.1161/01.res.88.3.325>.
- Just, S., Chenard, B.L., Ceci, A., Strassmaier, T., Chong, J.A., Blair, N.T., Gallaschun, R.J., Del Camino, D., Cantin, S., D'Amours, M., Eickmeier, C., Fanger, C.M., Hecker, C., Hessler, D.P., Hengerer, B., Kroker, K.S., Malekiani, S., Mihalek, R., McLaughlin, J., Moran, M.M., 2018. Treatment with HC-070, a potent inhibitor of TRPC4 and TRPC5, leads to anxiolytic and antidepressant effects in mice. *PLoS One* 13 (1), e0191225. <https://doi.org/10.1371/journal.pone.0191225>.
- Kerr, W.J., Morrison, A.J., Pazicky, M., Weber, T., 2012. Modified Shapiro reactions with bis(mesityl)magnesium as an efficient base reagent. *Org. Lett.* 14 (9), 2250–2253. <https://doi.org/10.1021/ol300652k>.
- Krishnan, P., Lee, F.-K., Yap, V.A., Low, Y.-Y., Kam, T.-S., Yong, K.-T., Ting, K.-N., Lim, K.-H., 2020. Schwarzinines A–G, 1,4-Diarylbutanoid–Phenethylamine Conjugates from the Leaves of *Ficus schwarzii*. *J. Nat. Prod.* 83 (1), 152–158. <https://doi.org/10.1021/acs.jnatprod.9b01160>.
- Kwan, H.Y., Huang, Y., Yao, X., 2004. Regulation of canonical transient receptor potential isoform 3 (TRPC3) channel by protein kinase G. *Proc. Natl. Acad. Sci. USA* 101 (8), 2625–2630. <https://doi.org/10.1073/pnas.0304471101>.
- Lee, F.K., Krishnan, P., Muhamad, A., Low, Y.Y., Kam, T.S., Ting, K.N., Lim, K.H., 2022. Concise synthesis of the vasorelaxant alkaloids schwarzinines A and B. *Nat. Prod. Res* 36 (15), 3972–3978. <https://doi.org/10.1080/14786419.2021.1903005>.
- Lee, R.Y., Lobel, L., Hengartner, M., Horvitz, H.R., Avery, L., 1997. Mutations in the alpha1 subunit of an L-type voltage-activated Ca<sup>2+</sup> channel cause myotonia in *Caenorhabditis elegans*. *Embo J.* 16 (20), 6066–6076. <https://doi.org/10.1093/emboj/16.20.6066>.
- Liang, M., Zhong, W., Miao, F., Wu, H., Liu, Y., 2018. Effects of losartan on vasomotor function and canonical transient receptor potential channels in the aortas of sinoaortic denervation rats. *Clin. Exp. Hypertens.* 40 (1), 39–48. <https://doi.org/10.1080/10641963.2017.1299746>.
- Lin, X.H., Hong, H.S., Zou, G.R., Chen, L.L., 2015. Upregulation of TRPC1/6 may be involved in arterial remodeling in rat. *J. Surg. Res* 195 (1), 334–343. <https://doi.org/10.1016/j.jss.2014.12.047>.
- Liu, D., Scholze, A., Zhu, Z., Kreutz, R., Wehland-von-Trebra, M., Zidek, W., Tepel, M., 2005. Increased transient receptor potential channel TRPC3 expression in spontaneously hypertensive rats. *Am. J. Hypertens.* 18 (11), 1503–1507. <https://doi.org/10.1016/j.amjhyper.2005.05.033>.
- Liu, D., Xiong, S., Zhu, Z., 2014. Imbalance and dysfunction of transient receptor potential channels contribute to the pathogenesis of hypertension. *Sci. China Life Sci.* 57 (8), 818–825. <https://doi.org/10.1007/s11427-014-4713-3>.
- Loga, F., Domes, K., Freichel, M., Flockerzi, V., Dietrich, A., Birnbaumer, L., Hofmann, F., Wegener, J.W., 2013. The role of cGMP/cGKI signalling and Trpc channels in regulation of vascular tone. *Cardiovasc Res* 100 (2), 280–287. <https://doi.org/10.1093/cvr/cvt176>.
- Loong, B.J., Tan, J.H., Lim, K.H., Mbaki, Y., Ting, K.N., 2015. Contractile function of smooth muscle retained after overnight storage. *Naunyn Schmiede Arch. Pharm.* 388 (10), 1061–1067. <https://doi.org/10.1007/s00210-015-1140-3>.
- Low, A.M., Kwan, C.Y., Daniel, E.E., 1992. Evidence for two types of internal Ca<sup>2+</sup> stores in canine mesenteric artery with different refilling mechanisms. *Am. J. Physiol. Heart Circ. Physiol.* 262 (1), H31–H37. <https://doi.org/10.1152/ajpheart.1992.262.1.H31>.
- Ludlow, M.J., Gaunt, H.J., Rubaiy, H.N., Musialowski, K.E., Blythe, N.M., Vasudev, N.S., Muraki, K., Beech, D.J., 2017. Englerin A-evoked Cytotoxicity Is Mediated by Na<sup>+</sup> Influx and Counteracted by Na<sup>+</sup>/K<sup>+</sup>-ATPase. *J. Biol. Chem.* 292 (2), 723–731. <https://doi.org/10.1074/jbc.M116.755678>.
- Mak, Y.-Y., Loong, B.-J., Millns, P., Bauer, C.C., Bon, R.S., Mbaki, Y., Lee, F.-K., Lim, K.-H., Kong, C., Then, S.-M., & Ting, K.-N. (2022). Schwarzinicine A inhibits transient receptor potential canonical channels and exhibits overt vasorelaxation effects [https://doi.org/10.1002/ptr.7489]. *Phytotherapy Research*, n/a(n/a). <https://doi.org/10.1002/ptr.7489>.
- Martin-Bórnez, M., Galeano-Otero, I., Del Toro, R., Smani, T., 2020. TRPC and TRPV Channels' Role in Vascular Remodeling and Disease. *Int. J. Mol. Sci.* 21 (17) <https://doi.org/10.3390/ijms21176125>.
- Minard, A., Bauer, C.C., Chuntharpursat-Bon, E., Pickles, I.B., Wright, D.J., Ludlow, M.J., Burnham, M.P., Warriner, S.L., Beech, D.J., Muraki, K., Bon, R.S., 2019. Potent, selective, and subunit-dependent activation of TRPC5 channels by a xanthine derivative. *Br. J. Pharm.* 176 (20), 3924–3938. <https://doi.org/10.1111/bph.14791>.
- Okada, T., Shimizu, S., Wakamori, M., Maeda, A., Kurosaki, T., Takada, N., Imoto, K., Mori, Y., 1998. Molecular cloning and functional characterisation of a novel receptor-activated TRP Ca<sup>2+</sup> channel from mouse brain. *J. Biol. Chem.* 273 (17), 10279–10287. <https://doi.org/10.1074/jbc.273.17.10279>.
- Panthiya, L., Pantan, R., Tocharus, J., Nakaew, A., Suksamran, A., Tocharus, C., 2019. Endothelin-dependent and endothelin-independent vasorelaxant effects of tiliacorinine 12'-O-acetate and mechanisms on isolated rat aorta. *Biomed. Pharm.* 109, 2090–2099. <https://doi.org/10.1016/j.bioph.2018.11.062>.
- Philipp, S., Hambrecht, J., Braslavski, L., Schroth, G., Freichel, M., Murakami, M., Cavalié, A., Flockerzi, V., 1998. A novel capacitative calcium entry channel expressed in excitable cells. *EMBO J.* 17 (15), 4274–4282. <https://doi.org/10.1093/emboj/17.15.4274>.
- Rubaiy, H.N., Ludlow, M.J., Henrot, M., Gaunt, H.J., Miteva, K., Cheung, S.Y., Tanahashi, Y., Hamzah, N., Musialowski, K.E., Blythe, N.M., Appleby, H.L., Bailey, M.A., McKeown, L., Taylor, R., Foster, R., Waldmann, H., Nussbaumer, P., Christmann, M., Bon, R.S., Beech, D.J., 2017. Picomolar, selective, and subtype-specific small-molecule inhibition of TRPC1/4/5 channels. *J. Biol. Chem.* 292 (20), 8158–8173. <https://doi.org/10.1074/jbc.M116.773556>.
- Schleifer, H., Doleschal, B., Lichtenegger, M., Oppenrieder, R., Derler, I., Frischauf, I., Glasnov, T.N., Kappe, C.O., Romanin, C., Groschner, K., 2012. Novel pyrazole compounds for pharmacological discrimination between receptor-operated and store-operated Ca(2+) entry pathways. *Br. J. Pharm.* 167 (8), 1712–1722. <https://doi.org/10.1111/j.1476-5381.2012.02126.x>.
- Senadheera, S., Kim, Y., Grayson, T.H., Toemoe, S., Kochukov, M.Y., Abramowitz, J., Housley, G.D., Bertrand, R.L., Chadha, P.S., Bertrand, P.P., Murphy, T.V., Tare, M., Birnbaumer, L., Marrelli, S.P., Sandow, S.L., 2012. Transient receptor potential canonical type 3 channels facilitate endothelium-derived hyperpolarisation-mediated resistance artery vasodilator activity. *Cardiovasc. Res.* 95 (4), 439–447. <https://doi.org/10.1093/cvr/cvs208>.
- Steger, K.A., Shtonda, B.B., Thacker, C., Snutch, T.P., Avery, L., 2005. The *C. elegans* T-type calcium channel CCA-1 boosts neuromuscular transmission. *J. Exp. Biol.* 208 (Pt 11), 2191–2203. <https://doi.org/10.1242/jeb.01616>.
- Tammaro, P., Smith, A.L., Hutchings, S.R., Smirnov, S.V., 2004. Pharmacological evidence for a key role of voltage-gated K<sup>+</sup> channels in the function of rat aortic smooth muscle cells. *Br. J. Pharmacol.* 143 (2), 303–317. <https://doi.org/10.1038/sj.bjp.0705957>.
- Thilo, F., Lodenkemper, C., Berg, E., Zidek, W., Tepel, M., 2009. Increased TRPC3 expression in vascular endothelium of patients with malignant hypertension. *Mod. Pathol.* 22 (3), 426–430. <https://doi.org/10.1038/modpathol.2008.200>.
- Tirupathi, C., Freichel, M., Vogel, S.M., Paria, B.C., Mehta, D., Flockerzi, V., Malik, A.B., 2002. Impairment of store-operated Ca<sup>2+</sup> entry in TRPC4(-/-) mice interferes with increase in lung microvascular permeability. *Circ. Res* 91 (1), 70–76. <https://doi.org/10.1161/01.res.000023391.40106.a8>.
- Trebak, M., Hempel, N., Wedel, B.J., Smyth, J.T., Bird, G.S., Putney, J.W., Jr, 2005. Negative regulation of TRPC3 channels by protein kinase C-mediated phosphorylation of serine 712. *Mol. Pharm.* 67 (2), 558–563. <https://doi.org/10.1124/mol.104.007252>.
- Vannier, B., Peyton, M., Boulay, G., Brown, D., Qin, N., Jiang, M., Zhu, X., Birnbaumer, L., 1999. Mouse trp2, the homologue of the human trpc2 pseudogene, encodes mTrp2, a store depletion-activated capacitative Ca<sup>2+</sup> entry channel. *Proc. Natl. Acad. Sci. USA* 96 (5), 2060–2064. <https://doi.org/10.1073/pnas.96.5.2060>.
- Wang, H., Cheng, X., Tian, J., Xiao, Y., Tian, T., Xu, F., Hong, X., Zhu, M.X., 2020. TRPC channels: Structure, function, regulation and recent advances in small molecular probes. *Pharm. Ther.* 209, 107497. <https://doi.org/10.1016/j.pharmthera.2020.107497>.
- Wes, P.D., Chevesich, J., Jeromin, A., Rosenberg, C., Stetten, G., Montell, C., 1995. TRPC1, a human homolog of a *Drosophila* store-operated channel. *Proc. Natl. Acad. Sci. USA* 92 (21), 9652–9656. <https://doi.org/10.1073/pnas.92.21.9652>.
- Zhu, Y., Gao, M., Zhou, T., Xie, M., Mao, A., Feng, L., Yao, X., Wong, W.T., Ma, X., 2019. The TRPC5 channel regulates angiogenesis and promotes recovery from ischemic injury in mice. *J. Biol. Chem.* 294 (1), 28–37. <https://doi.org/10.1074/jbc.RA118.005392>.